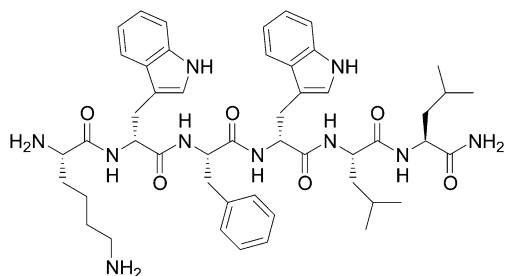




positively charged amino acid Lys at the N-terminus led to a potent inverse agonist (Figure 1). In contrast, addition of the



**Figure 1.** The ghrelin receptor ligand KwFwLL-NH<sub>2</sub> can be easily modulated to act as a potent inverse agonist or a potent agonist, depending on only minor changes in the peptide sequence.

neutral amino acid Ala revealed a potent agonist.<sup>23</sup> The aromatic core wFw motif appeared to be crucial for receptor binding.<sup>22</sup> Finally, the lead peptide KwFwLL-NH<sub>2</sub> acted as a specific inverse agonist at the ghrelin receptor but with moderate potency and low efficacy.

In this manuscript, an intensive structure–activity relationship study of the lead peptide revealed a tripeptide switch region able to induce agonism or inverse agonism. The influence of amino acid aromaticity, size, and orientation was investigated at the tripeptide region to determine the characteristics of the switch. The most potent inverse agonists and agonists, which exhibit only small differences in their structures, emphasized the sensitivity of the switch region. Mutagenesis studies were performed in parallel to investigate key positions at the receptor site inducing agonistic or inverse agonistic response. In addition, binding and modeling studies were carried out to determine key interactions between the peptide and the receptor. Finally, preliminary *in vivo* studies of the inverse agonist could evaluate its influence on food intake.

## RESULTS

### Peptide Synthesis of KwFwLL-NH<sub>2</sub> Analogues.

KwFwLL-NH<sub>2</sub> analogues were synthesized by automated solid phase peptide synthesis.<sup>24</sup> Non-natural amino acids to modify the peptide core wFw were introduced manually and are summarized in Figure 2. Peptide identity was confirmed by MALDI-TOF MS and peptide purity by RP-HPLC on two different columns. All peptides were obtained with high purity (>95%) (Supporting Information Table S1).

**Substitution of D-Trp<sup>2</sup> Revealed Highly Potent Inverse Agonists.** Nine analogues (2–11) with the sequence KxFwLL-NH<sub>2</sub> (Table 1) were synthesized and tested for potency and efficacy, i.e., the behavior as agonists or inverse agonists in an inositol trisphosphate turnover assay with COS7 cells transfected with the ghrelin receptor (Figure 3a). We used the inositol trisphosphate turnover assay for evaluating agonism and inverse agonism due to the signaling of the ghrelin receptor over G<sub>αq/11</sub> pathway. The IP<sub>3</sub> turnover assay is well established for the receptor and can be used to characterize the constitutive activity, which is an important feature in context with peptide design for the ghrelin receptor.

The efficacy of the peptides was determined from the difference between the constitutive activity and the activity level at highest peptide concentration; i.e., the decrease or increase of constitutive activity was evaluated. The unmodified hexapeptide (peptide 2) is an inverse agonist and showed an efficacy of 37% and an EC<sub>50</sub> of 45.6 nM, which is in agreement with previous reports.<sup>23</sup> In general, substitution of D-Trp<sup>2</sup> with chosen D-amino acids in the core peptide maintained inverse agonistic activity. The most potent inverse agonists were found by substitution of D-Trp<sup>2</sup> with D-1-Nal (3, EC<sub>50</sub> = 3.4 ± 0.4 nM), D-Bth (4, EC<sub>50</sub> = 5.7 ± 1.7 nM), and D-Dip (5, EC<sub>50</sub> = 13.1 ± 1.9 nM). Those peptides were highly active and exhibited a potency up to 13.4-fold higher than the lead peptide KwFwLL-NH<sub>2</sub> (2). Peptides 6 (D-2-Nal), 7 (D-Bpa), 8 (D-Bip),

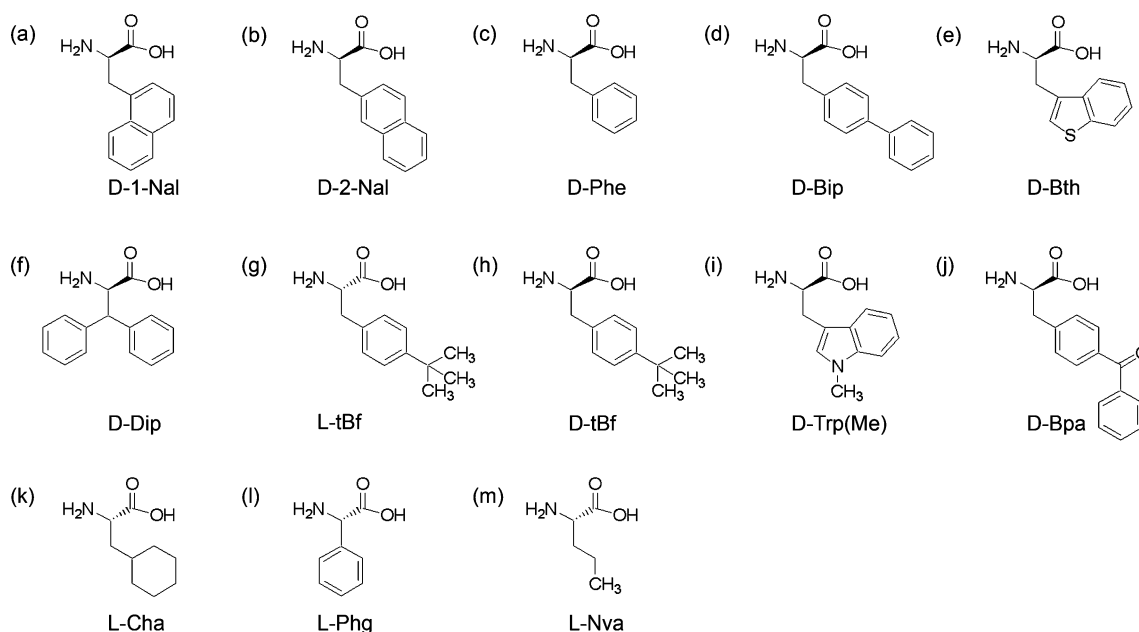


**Figure 2.** Chemical structures of non-proteinogenic amino acids used to synthesize analogues of KwFwLL-NH<sub>2</sub>: (a) 1-naphthyl-D-alanine (D-1-Nal), (b) 2-naphthyl-D-alanine (D-2-Nal), (c) D-phenylalanine (D-Phe), (d) 4,4'-biphenyl-D-alanine (D-Bip), (e)  $\beta$ -(3-benzothieryl)-D-alanine (D-Bth), (f) 3,3-diphenyl-D-alanine (D-Dip), (g) *tert*-butyl-L-phenylalanine (L-tBf), (h) *tert*-butyl-D-phenylalanine (D-tBf), (i) *N*-methyl-D-tryptophane (D-Trp(Me)), (j) 4-benzoyl-D-phenylalanine (D-Bpa), (k) cyclohexyl-L-alanine (L-Cha), (l) L-phenylglycine (L-Phg), and (m) L-norvaline (L-Nva).

Table 1. Inositol Trisphosphate Turnover Assay of KwFwLL-NH<sub>2</sub> Analogues<sup>a</sup>

compd	peptide	EC <sub>50</sub> ± SEM [nM]	<i>x</i> -fold (EC <sub>50</sub> )	E <sub>max</sub> ± SEM [Δ%]	<i>x</i> -fold (E <sub>max</sub> )	<i>n</i>	behavior
1	ghrelin	1.4 ± 0.2		162 ± 12		8	agonist
2	KwFwLL-NH <sub>2</sub>	45.6 ± 5.4		37 ± 5		3	inverse agonist
3	K-(D-1-Nal)-FwLL-NH <sub>2</sub>	3.4 ± 0.4	0.07	64 ± 2	1.7	5	inverse agonist
4	K-(D-Bth)-FwLL-NH <sub>2</sub>	5.7 ± 1.7	0.13	81 ± 2	2.2	5	inverse agonist
5	K-(D-Dip)-FwLL-NH <sub>2</sub>	13.1 ± 1.9	0.29	87 ± 2	2.4	4	inverse agonist
6	K-(D-2-Nal)-FwLL-NH <sub>2</sub>	161.3 ± 32.1	3.54	66 ± 4	1.8	2	inverse agonist
7	K-(D-Bpa)-FwLL-NH <sub>2</sub>	168.6 ± 36.3	3.70	67 ± 7	1.8	4	inverse agonist
8	K-(D-Bip)-FwLL-NH <sub>2</sub>	183.7 ± 97.8	4.03	82 ± 0	2.2	3	inverse agonist
9	K-(D-Phe)-FwLL-NH <sub>2</sub>	240.9 ± 129.1	5.28	62 ± 4	1.7	5	inverse agonist
10	K-(D-tBf)-FwLL-NH <sub>2</sub>	624.4 ± 326.9	13.7	76 ± 5	2.1	4	inverse agonist
11	K-(D-Trp(Me))-FwLL-NH <sub>2</sub>	>1000	>20			2	
12	K-(D-1-Nal)-(L-Cha)-wLL-NH <sub>2</sub> <sup>b</sup>	96.8 ± 33.5	28.5	85 ± 3	1.3	3	inverse agonist
13	K-(D-1-Nal)-(D-Phe)-wLL-NH <sub>2</sub> <sup>b</sup>	119.6 ± 15.8	35.2	58 ± 7	0.9	4	inverse agonist
14	K-(D-1-Nal)-(L-tBf)-wLL-NH <sub>2</sub> <sup>b</sup>	124.1 ± 47.4	36.5	84 ± 3	1.3	3	inverse agonist
15	K-(D-1-Nal)-(L-Nva)-wLL-NH <sub>2</sub> <sup>b</sup>	498.1 ± 250.9	147	71 ± 4	1.1	3	inverse agonist
16	K-(D-1-Nal)-(L-Phg)-wLL-NH <sub>2</sub> <sup>b</sup>	>1000	>290			2	
17	KwF-(D-2-Nal)-LL-NH <sub>2</sub> <sup>c</sup>	12.6 ± 2.2	9.00	156 ± 22	1	3	agonist
18	KwF-(D-1-Nal)-LL-NH <sub>2</sub> <sup>c</sup>	17.9 ± 6.4	12.8	54 ± 10	0.3	3	agonist
19	KwF-(D-Bip)-LL-NH <sub>2</sub> <sup>c</sup>	>1000	>700			2	
20	KwF-(D-Bpa)-LL-NH <sub>2</sub> <sup>c</sup>	>1000	>700			2	
21	KwF-(D-Dip)-LL-NH <sub>2</sub> <sup>c</sup>	>1000	>700			4	
22	KwF-(D-Bth)-LL-NH <sub>2</sub> <sup>c</sup>	>1000	>700			3	
23	K-(D-1-Nal)-F-(D-1-Nal)-LL-NH <sub>2</sub>	>1000	>20			2	
24	K-(D-1-Nal)-F-(D-Bth)-LL-NH <sub>2</sub>	2.1 ± 0.6	0.05	40 ± 2	1.1	2	inverse agonist
25	K-(D-Bth)-F-(D-Bth)-LL-NH <sub>2</sub>	9.4 ± 2.6	0.21	67 ± 2	1.8	2	inverse agonist

<sup>a</sup>EC<sub>50</sub> and E<sub>max</sub> of the peptides at the ghrelin receptor are listed with respect to inverse agonistic or agonistic activity, depending on peptide characteristics. EC<sub>50</sub> and E<sub>max</sub> are listed as the mean value ± SEM of *n* experiments. *x*-fold indicates the shift in EC<sub>50</sub> or efficacy of the hexapeptides compared to KwFwLL-NH<sub>2</sub>, if not indicated otherwise. <sup>b</sup>*x*-fold shift compared to peptide 3 <sup>c</sup>*x*-fold shift compared to ghrelin.

and 9 (D-Phe) presented a moderate activity with EC<sub>50</sub> values between 161.3 and 240.9 nM. Substitution of D-Trp<sup>2</sup> with D-tBf (10, EC<sub>50</sub> = 624.4 ± 326.9 nM) resulted in a peptide showing a severe loss of potency, and introduction of D-Trp(Me) (11, EC<sub>50</sub> > 1000 nM) led to an inactive compound. The efficacy of the inverse agonists was significantly increased by all modifications except D-Trp(Me). Notably, peptides 4, 5, and 8 exhibited an efficacy higher than 80%.

**L-Phe<sup>3</sup> Is Important for the Potency of the Hexapeptides.** The significance of the aromatic character at position 3 was evaluated on the optimized ghrelin receptor inverse agonist K-(D-1-Nal)-FwLL-NH<sub>2</sub> (3). Five analogues with the sequence K-(D-1-Nal)-zwLL-NH<sub>2</sub> were synthesized (Table 1). In general, a decrease in potency could be observed in comparison to the lead peptide 3. Surprisingly, efficacy was maintained or increased.

The exchange of L-Phe at position 3 with its D-analogue (D-Phe, 13) resulted in a 35.2-fold loss of activity, but no significant difference in efficacy was observed (Figure 3b). In contrast, the introduction of L-tBf (peptide 14) significantly increased efficacy (E<sub>max</sub> = 84%) but also had a negative influence on potency. Thus, the additional *tert*-butyl group in para-position at the aromatic benzene ring influenced efficacy and activity. The introduction of L-Phg (peptide 16) resulted in a total loss of activity with an EC<sub>50</sub> higher than 1000 nM.

The replacement of L-Phe<sup>3</sup> with the aliphatic amino acids L-Cha (12) and L-Nva (15) decreased potency in both cases. Peptide 12 presented an EC<sub>50</sub> of 96.8 nM and efficacy of 85%. Substitution with L-Nva (15) led to a peptide with very low potency (EC<sub>50</sub> = 498.1 nM).

**Substitution of D-Trp<sup>4</sup> in the wFw-core Eliminates Inverse Agonistic Activity.** Surprisingly, replacement of D-Trp residue at position 4 with various aromatic D-amino acids eliminated inverse agonistic activity (Table 1). Introduction of D-Bip (19), D-Bpa (20), D-Dip (21), and D-Bth (22) suppressed the potency at the ghrelin receptor. Moreover, introduction of both D-2-Nal (17) and D-1-Nal (18) at position 4 led to highly potent agonists with EC<sub>50</sub> values of 12.6 and 17.9 nM, respectively. Interestingly, peptide 17 containing D-2-Nal exhibited a significantly higher E<sub>max</sub> than peptide 18 containing D-1-Nal (efficacy of 156% versus 54%), comparable to the endogenous ligand ghrelin (Figure 3c).

**Simultaneous Exchange of D-Trp<sup>2,4</sup> by D-1-Nal Resulted in a Total Loss of Efficacy.** For further investigations, the hexapeptide was modified simultaneously on D-Trp at positions 2 and 4, with either D-1-Nal or D-Bth. Three analogues with the sequence KxFyLL-NH<sub>2</sub> were synthesized (Table 1). Remarkably, substitution with D-1-Nal at both positions (23) totally suppressed activity (Figure 4a). In contrast, the introduction of D-Bth at position 4 (24) or at both positions (25) led to highly potent inverse agonists with EC<sub>50</sub> values of 2.1 and 9.4 nM, respectively. Peptide 24 showed an efficacy of 40%; the presence of D-Bth at positions 2 and 4 (25) led to a more efficient peptide (E<sub>max</sub> = 67%).

**Competitive Binding Assay Revealed High Affinity for the Inverse Agonist.** Receptor binding affinities of ghrelin (1), K-(D-1-Nal)-FwLL-NH<sub>2</sub> (3), KwF-(D-1-Nal)-LL-NH<sub>2</sub> (18), and K-(D-1-Nal)-F-(D-1-Nal)-LL-NH<sub>2</sub> (23) and peptides showing no potency in signal transduction were tested in competitive binding studies with <sup>125</sup>I-His-ghrelin (Table 2). Interestingly, the three hexapeptides containing D-1-Nal

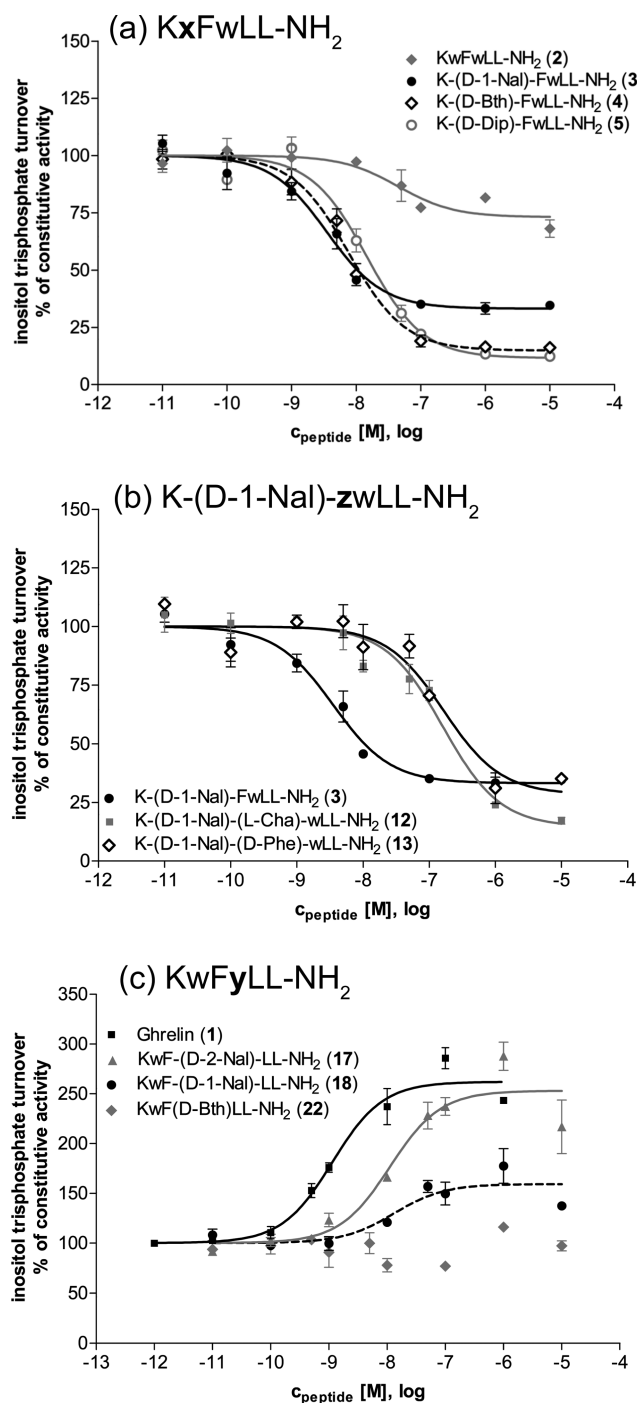


**Figure 3.** Structure–activity relationship studies of the aromatic peptide core. (a) Substitutions of D-Trp<sup>2</sup> with aromatic amino acids resulted in hexapeptides with increased potency and efficacy. (b) In contrast, substitution of L-Phe<sup>3</sup> with aromatic, aliphatic, or cyclic amino acids led to less potent peptides, highlighting the importance of this amino acid on peptide potency. (c) Introduction of D-1-Nal and D-2-Nal at position 4 of KwFwLL-NH<sub>2</sub> turned the peptide into an agonist. Efficacy of peptide 17 is comparable to that of the endogenous ligand ghrelin (1).

showed different affinities, although they are structurally very similar. Whereas the inverse agonist 3 is able to compete with ghrelin with a  $K_i$  of 4.9 nM, the agonist 18 displays a much lower  $K_i$ . Interestingly, the binding of peptide 23 that showed neither agonistic nor inverse agonistic behavior in the

functional assay is between the inverse agonist and the agonist with a  $K_i$  of 34.9 nM (Figure 4b). Peptides exhibiting no potency in activity assay were also tested for displacement of ghrelin. Therefore, we investigated the binding first at  $10^{-6}$  and  $10^{-8}$  M. At this concentration, peptides 19, 20, and 21 did not show any displacement at  $10^{-8}$  M and a displacement with less than 50% at  $10^{-6}$  M, indicating  $IC_{50} \geq 1000$  nM (Figure 4c). Peptides 11 and 22 showed a displacement at  $10^{-6}$  M and were tested further. For peptide 11, a  $K_i$  of 22.1 nM was found. For peptide 22, a  $K_i$  of 31.3 nM was found. Binding affinity of peptide 17 is comparable to that of peptide 18.

**Mutagenesis of Phe119 Removes Inverse Agonistic Activity of K-(D-1-Nal)-FwLL-NH<sub>2</sub>, but Agonist Behavior of KwF-(D-2-Nal)-LL-NH<sub>2</sub> Is Maintained.** Substitution of position 119 (PheIII:04) and position 123 (SerIII:08) of the ghrelin receptor was created by mutagenesis (Table 3). Expression level of all mutants was comparable to wild type receptor expression. Most of the Phe119 mutations eliminated the activity of the inverse agonist. However, mutation of Phe119 with Ser changed the efficacy of K-(D-1-Nal)-FwLL-NH<sub>2</sub> (3) from an inverse agonist to an agonist with an  $EC_{50}$  of 237.6 nM. Mutation of Ser123 with different amino acids did not induce agonism, but Ser123:Ala and Ser123:Trp resulted in receptors that cannot be influenced by the inverse agonist. Remarkably, both Phe119:Ser and Ser123:Ala did not influence the behavior of the agonist KwF-(D-2-Nal)-LL-NH<sub>2</sub> (17).

**Modeling Indicates L-Shaped Form for the Hexapeptides.** For computational modeling of the ghrelin receptor–ligand interaction we selected the inverse agonists KwFwLL-NH<sub>2</sub> (2), K-(D-1-Nal)-FwLL-NH<sub>2</sub> (3), and K-(D-Dip)-FwLL-NH<sub>2</sub> (5) and the agonists KwF-(D-2-Nal)-LL-NH<sub>2</sub> (17) and KwF-(D-1-Nal)-LL-NH<sub>2</sub> (18). The resulting top scoring docking poses of 2, 3, 5, 17, and 18 to the receptor ensemble identified a small number of receptor variants, which could accommodate the five peptides in a similar docking pose, in which the L-shaped N-terminus of the ligands fitted nicely into the complementary binding pocket of the ghrelin receptor. In general, these receptor variants were characterized by an open binding pocket in which the extracellular loop (ECL) 2b adopts an  $\alpha$ -helical conformation. In this mode, the corresponding motifs K-(D-Trp, D-1-Nal, D-Dip)-F-(D-Trp, D-1-Nal, D-2-Nal) extend down into the binding pocket to perform aromatic hydrophobic interactions with the aromatic cluster of residues located at the interface of TM-VI and TM-VII (shown exemplarily for peptide 3 in Figure 5). In particular, the positively charged aliphatic lysine side chain in the N-terminal part that is common to all the studied ligands is involved in charge–charge interactions with the carboxyl acid side chain of Glu124, which we previously have identified to be an important anchor point for a variety of small molecule and peptide ligands.<sup>25,26</sup> Further, the aromatic indole side chain, D-1-Nal and D-Dip in the second position of 2, 3, 5, 17, and 18 are positioned in a lower aromatic pocket, making aromatic–aromatic edge-to-face and aromatic–aromatic stacking interactions with Phe279, Phe309, and 312 as well as hydrophobic interactions with Leu100, whereas the Phe side chain in the third position interacts with Phe286. In this mode, the backbone amides are positioned to make hydrogen bond interactions with Arg283 and Gln120 and with Glu202 in ECL-2b, which all point into the binding pocket, while the aliphatic side chains corresponding to the conserved LL-NH<sub>2</sub> motif are involved in hydrophobic aromatic interactions with residues in ECL-2b and ECL-1. This binding pose is in good agreement



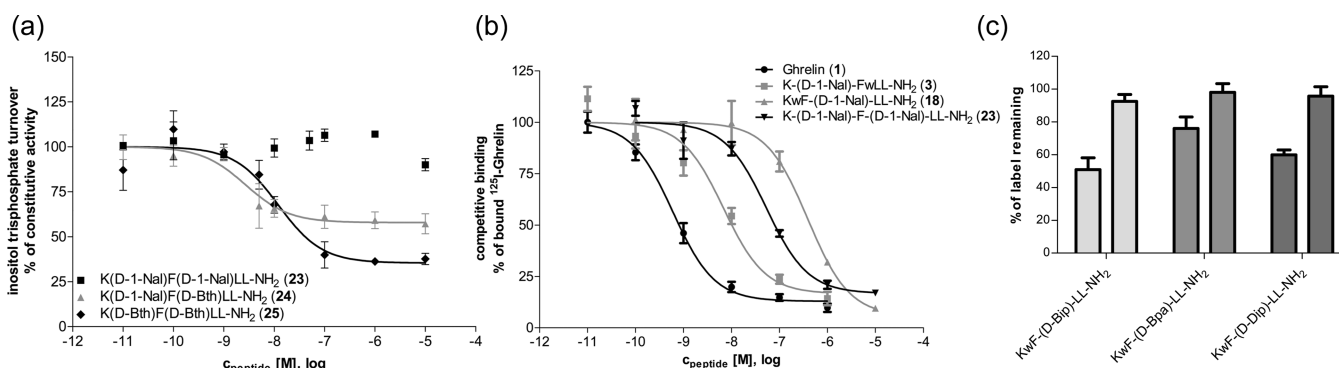


**Figure 4.** (a) Sigmoidal concentration–response curves of peptides 23, 24, and 25 from an IP<sub>3</sub> turnover assay. Substitution with 1-naphthyl-D-alanine at both positions (23) led to a significant loss of efficacy. Peptides containing β-(3-benzothienyl)-D-alanine (24, 25) maintain inverse agonistic activity, with higher potency and/or efficacy than KwFwLL-NH<sub>2</sub>. (b) Competition binding assay of the D-1-Nal containing peptides. The inverse agonist K-(D-1-Nal)-FwLL-NH<sub>2</sub> (3) showed the highest affinity to the ghrelin receptor. (c) Nonpotent peptides were tested for binding displacement. For 19, 20, and 21, IC<sub>50</sub> ≥ 1000 nM could be observed.

**Table 2. Competition Binding Assays<sup>a</sup>**

compd	peptide	K <sub>i</sub> ± SEM [nM]	x-fold	n
1	ghrelin	0.7 ± 0.2		4
3	K-(D-1-Nal)-FwLL-NH <sub>2</sub>	4.9 ± 0.8	7.00	2
11	K-(D-Trp(Me))-FwLL-NH <sub>2</sub>	22.1 ± 3.0	31.6	2
17	KwF-(D-2-Nal)-LL-NH <sub>2</sub>	234.2 ± 82.7	335	2
18	KwF-(D-1-Nal)-LL-NH <sub>2</sub>	247.2 ± 79.4	353	2
22	KwF-(D-Bth)-LL-NH <sub>2</sub>	31.3 ± 0.0	44.7	2
23	K-(D-1-Nal)-F-(D-1-Nal)-LL-NH <sub>2</sub>	34.9 ± 9.5	49.9	2

<sup>a</sup>K<sub>i</sub> is indicated as the mean value ± SEM of *n* experiments. *x*-fold indicates the shift in K<sub>i</sub> of the hexapeptides to ghrelin.

with mutational mapping of the related wFwLL-NH<sub>2</sub> pentapeptide.<sup>25</sup>

Furthermore, the hexapeptides showed the L-shaped form that was described for wFwLL-NH<sub>2</sub> in Holst et al.<sup>23</sup> Additionally, Lys<sup>1</sup>, Xaa<sup>2</sup>, and Phe<sup>3</sup> are more conformationally constrained, whereas Xaa<sup>4</sup> and both leucine residues Leu<sup>5</sup> and Leu<sup>6</sup> at the C-terminus have a higher degree of freedom (Figure 6).

The comparison of the five models showed only minor differences. Ser217 that showed no interaction with peptide 3 may interact with peptide 2 at the Lys side chain. The same could be observed for peptide 18. Both peptides contain a D-Trp at position 2. Interestingly, this could not be observed for KwF-(D-2-Nal)-LL-NH<sub>2</sub> (17). Furthermore, Leu103, which is also near the aromatic amino acid at position 2, likely interacts with peptides 2, 3, 17, and 18 but does not seem to interact with peptide 5; instead this peptide may interact with Leu306 at D-Dip<sup>2</sup>. Because of its space-consuming D-2-Nal residue at position 4, peptide 17 may interact with Ser289 and Ile297.

**K-(D-1-Nal)-FwLL-NH<sub>2</sub> Decreases Acute Food Intake Almost 5-Fold.** After showing the high constitutive activity of the receptor in vivo,<sup>11</sup> we tested one of the most potent inverse agonists for possible decrease of food intake due to a reduced constitutive activity to prove the concept. Compound 3 served as the prototype for the peptide series and was chosen for the assay. K-(D-1-Nal)-FwLL-NH<sub>2</sub> (peptide 3) presented an EC<sub>50</sub> of 3.4 nM and an efficacy of 64%, and an affinity of 4.9 nM was tested. Since there is a high identity between human and rat ghrelin receptor (>95%) and since the activity of the peptide 3 was identical in human and rodent receptors, rats are a good choice for first in vivo assays. Rats were injected with peptide 3

**Table 3. Mutagenesis Studies of Phe119 and Ser123<sup>a</sup>**

compd	peptide	mutant	expression level ± SEM [%]	EC <sub>50</sub> ± SEM [nM]	E <sub>max</sub> ± SEM [%]	n	behavior
3	K-(D-1-Nal)-FwLL-NH <sub>2</sub>	WT	1.0 ± 0.0	3.8 ± 1.4	68 ± 7	7	inverse agonist
		Phe119:Ser	1.2 ± 0.2	237.6 ± 38.5	178 ± 37	5	agonist
		Phe119:His	1.1 ± 0.0	>1000		3	
		Phe119:Val	1.1 ± 0.1	>1000		3	
		Phe119:Tyr	1.3 ± 0.4	2.8 ± 1.7	82 ± 9	3	inverse agonist
		Phe119:Ala	1.1 ± 0.2	>1000		3	
		Ser123:Ala	1.2 ± 0.1	>1000		7	
		Ser123:Asp	1.1 ± 0.2	3.3 ± 1.3	68 ± 2	3	inverse agonist
		Ser123:Thr	1.1 ± 0.2	7.2 ± 2.7	82 ± 2	2	inverse agonist
		Ser123:Val	1.1 ± 0.2	11.2 ± 3.8	64 ± 3	3	inverse agonist
		Ser123:Trp	1.2 ± 0.2	>1000		3	
17	KwF-(D-2-Nal)-LL-NH <sub>2</sub>	WT	1.0 ± 0.0	7.2 ± 2.7	137 ± 31	4	agonist
		Phe119:Ser	1.2 ± 0.2	13.4 ± 8.6	160 ± 15	2	agonist
		Ser123:Ala	1.2 ± 0.1	6.7 ± 2.9	74 ± 6	2	agonist

<sup>a</sup>Expression of the mutants was studied by cell surface ELISA as fraction of wild type receptor expression in three independent experiments. EC<sub>50</sub> and E<sub>max</sub> are indicated as the mean value ± SEM of *n* experiments.

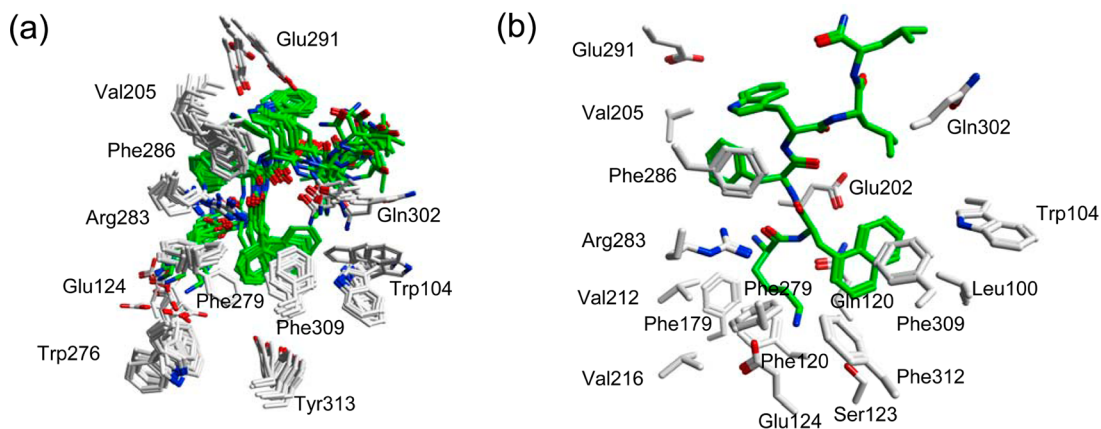


**Figure 5.** Proposed binding pocket and receptor–ligand interaction sides for the most potent inverse agonist K-(D-1-Nal)-FwLL-NH<sub>2</sub>, where (a) shows superimposed binding pocket for the inverse agonist and (b) gives an idea of interactions of the peptide with the receptor binding pocket in more detail.

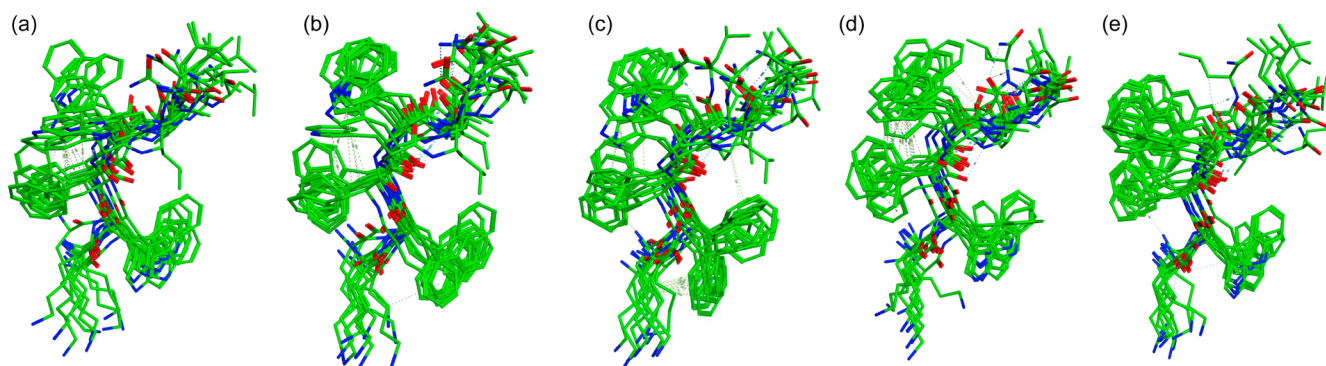


**Figure 6.** Conformations of the inverse agonists (a) KwFwLL-NH<sub>2</sub> (2), (b) K-(D-1-Nal)-FwLL-NH<sub>2</sub> (3), and (c) K-(D-Dip)-FwLL-NH<sub>2</sub> (5) and agonists (d) KwF-(D-1-Nal)-LL-NH<sub>2</sub> (18) and (e) KwF-(D-2-Nal)-LL-NH<sub>2</sub> (17).

(1 nmol/rat,  $n = 6$ ) intracerebroventricularly, and food intake was detected over 120 min. It could be shown that the inverse agonist was able to modulate food intake in rats (Figure 7),

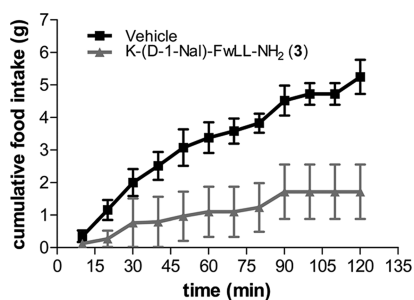


**Figure 7.** Study of acute food intake of rats in vivo. The peptide with the highest potency and affinity, K-(D-1-Nal)-FwLL-NH<sub>2</sub> (3), could decrease food intake almost 5-fold compared to vehicles.

resulting in an almost 5-fold decreased food intake compared to rats injected with the vehicle solution (0.9% saline with DMSO,  $n = 7$ ),  $P = 0.0077$ , two-way ANOVA. Additional effects of the animals included decreased activity and a decrease in water consumption.

## DISCUSSION AND CONCLUSION

The ghrelin receptor possesses a high constitutive activity assumed to have a major influence on food intake, energy

expenditure, and energy homeostasis.<sup>3,4,21,27</sup> This basal activity can be modulated by inverse agonists and agonists. Thereby, ghrelin receptor agonists could be a great alternative to ghrelin for the treatment of cachexia and anorexia. In contrast, potent inverse agonists could lead to antiobesity drugs.<sup>17,28–30</sup>

The hexapeptide KwFwLL-NH<sub>2</sub> behaves as an inverse agonist at the ghrelin receptor with moderate potency (45.6 nM) and low efficacy (37%). In the present study, we developed highly potent analogues of the hexapeptide acting as agonists or inverse agonists at the receptor. Substitution was performed at the aromatic core wFw, responsible for the binding and the peptide behavior. The replacement of D-Trp<sup>2</sup> with the non-proteinogenic amino acids D-1-Nal (3), D-Bth (4) and D-Dip (5) increased inverse agonist potency. The naphthalene and benzothienyl side chains are structurally close, but the ring sizes are slightly bigger than the indole of D-Trp. The structure of 3,3-diphenyl-D-alanine (D-Dip) differs notably from those of the other amino acids, since the two rings are not fused, resulting in a bigger and more flexible side chain. Peptide 5 showed a high potency and the highest efficacy observed for the tested inverse agonists. These structural differences may be responsible for the increase in efficacy and potency. Other substitutions at this position resulted in a decrease of potency, probably due to reduced interactions between ligand and receptor. Substitution of L-Phe<sup>3</sup> in the ghrelin receptor inverse agonist K-(D-1-Nal)-FwLL-NH<sub>2</sub> with hydrophobic amino acids led to inverse agonists with significant decreased activity. Therefore, the phenylalanine seems to be the

optimal choice at this position. These results agree with the first data of Holst et al. of the initially developed inverse agonist modified from substance P, where substitution of the Phe with Ala at the same position led to a dramatic loss of activity.<sup>22</sup> Furthermore, position 4 of the hexapeptide appeared critical for the peptide behavior. Introduction of D-2-Nal and D-1-Nal led to potent ghrelin receptor agonists (peptides 17 and 18, respectively). The efficacy of K-(D-2-Nal)-FwLL-NH<sub>2</sub> is notably higher, probably because of the conformation of D-2-Nal that is more space-consuming than D-1-Nal. Hence, minor changes in the aromatic core wFw, especially at positions 2 and 4, switch the ligand behavior from an inverse agonistic to an agonistic response (efficacy switch).

To characterize the switch region more precisely, peptides were synthesized with D-Bth and/or D-1-Nal at both positions 2 and 4 and led to the inverse agonistic acting peptides K-(D-1-Nal)-F-(D-Bth)-LL-NH<sub>2</sub> (24) and K-(D-Bth)-F-(D-Bth)-LL-NH<sub>2</sub> (25) and one peptide showing no activity (K-(D-1-Nal)-F-(D-1-Nal)-LL-NH<sub>2</sub>, 23). To summarize, introduction of D-1-Nal (3) and D-Bth (4) at position 2 led to strong inverse agonists with efficacies of 64% and 81%, respectively. Introduction of D-1-Nal at position 4 (18) resulted in a potent agonist with nanomolar activity. Substitution of D-Trp<sup>4</sup> with D-Bth (22) led to a total loss of activity. Accordingly, inverse agonistic and agonistic behavior can be neutralized and depends on the introduced amino acids. Figure 8 highlights the peptide

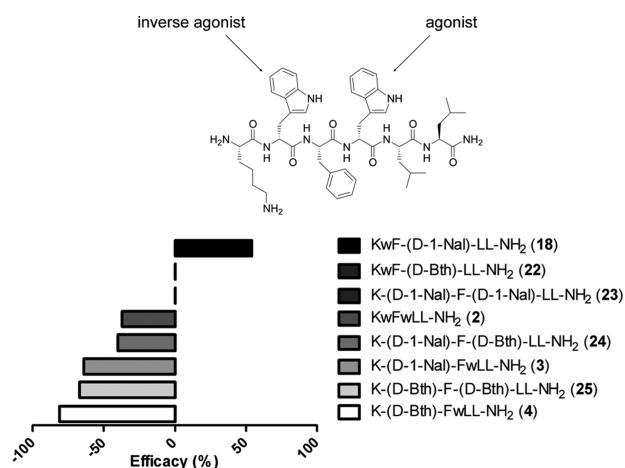


**Figure 8.** Efficacy values of peptides containing D-1-Nal and D-Bth. It is possible to create a chart of efficacy depending on the positions of the peptides, where these amino acids are inserted.

response based on the key modifications at positions 2 and 4. D-Bth clearly appeared to have a stronger inverse agonist effect at position 2 than D-1-Nal and D-Trp. In contrast, D-1-Nal presents a stronger agonist effect at position 4. Moreover, the lack of response observed for peptide 23 could be explained by a balance between the inverse agonist effect of D-1-Nal at position 2 and the agonist effect of D-1-Nal at position 4; i.e., the combination of agonist and inverse agonist results in a neutral ligand.

Interestingly, the inverse agonist K-(D-1-Nal)-FwLL-NH<sub>2</sub> (3) shows a strong binding affinity, whereas the agonist KwF-(D-1-Nal)-LL-NH<sub>2</sub> (18) presents only a low affinity to the receptor. K-(D-1-Nal)-F-(D-1-Nal)-LL-NH<sub>2</sub> (23) shows an intermediate binding affinity. Thus, D-1-Nal at position 2 (peptide 3) favored the inverse agonistic response with a strong binding at the receptor. In contrast, D-1-Nal at position 4 (peptide 18) favored

the agonistic response with a poor binding at the receptor. Moderate binding affinity of K-(D-1-Nal)-F-(D-1-Nal)-LL-NH<sub>2</sub> (23) can be seen as the balance of peptides 3 and 18.

The binding affinity was also tested for peptides that did not show any activity in the functional assay and for KwF-(D-2-Nal)-LL-NH<sub>2</sub> (17), which is the most potent and efficient agonist in this study. Binding of peptide 17 is comparable to that of peptide 18, emphasizing the hypothesis that the combination of agonist and inverse agonist properties within the same ligand leads to a neutral compound. Therefore, peptides 19, 20, and 21 did not exhibit displacement of <sup>125</sup>I-ghrelin with less than 1000 nM. In contrast, KwF-(D-Bth)-LL-NH<sub>2</sub> (22) and K-(D-Trp(Me))-FwLL-NH<sub>2</sub> (11) showed good binding with 31.3 and 22.1 nM, respectively. Peptide 22 showed a significantly higher binding affinity than peptide 18, and peptide 11 showed a lower binding affinity than peptide 3. This shows that these small modifications in the amino acid side chain affect not only the function of the peptides but also the affinity to the receptor. The binding affinities of peptides 11, 22, and 23 in the low nanomolar range combined with their poor potency at the receptor are truly interesting. These peptides should be characterized in more detail in the future to evaluate their antagonism at the ghrelin receptor or to investigate other signaling pathways, e.g., SRE signaling or  $\beta$ -arrestin mediated signaling.

The most potent hexapeptide is the inverse agonist K-(D-1-Nal)-FwLL-NH<sub>2</sub> (3). Acute food intake studies in vivo revealed a high potency to decrease food intake, and thereby, the peptide could be an important step in the development of antiobesity drugs. Nevertheless, adverse effects have to be evaluated in the future. Currently, a decrease in activity and in water consumption was monitored. As ghrelin itself leads to an increase in activity, the decrease is expected and accounts for a specific activity of the inverse agonist. It is known that the administration of ghrelin to cancer patients decreases nausea.<sup>31</sup> Therefore, cytotoxic effects or nausea cannot completely be ruled out, although strong nausea usually leads to an increase in water consumption, whereas we see a decrease. Ghrelin and the ghrelin receptor are also involved in other functions like learning and memory, stress induced depression, or alcohol abuse.<sup>32–34</sup> By now, the correlation between those functions and the inverse agonists are unclear, but there is a great interest to study these relations in order to get more information in the inverse agonist function and to reduce side effects.

Computational modeling of the ghrelin receptor was performed with the inverse agonists 2, 3, and 5 and the agonists 17 and 18 in order to evaluate the main ligand–receptor interactions and the key positions responsible for the constitutive activity. Although the compounds show different behavior, computational modeling of the hexapeptides in the receptor binding pocket led to only minor differences between the location of the inverse agonists and the agonists, suggesting interactions of different intensity. In contrast to the previous suggested binding mode for wFwLL-NH<sub>2</sub> and wFw-(Isn)-NH<sub>2</sub>, the aromatic peptide core of all hexapeptides does not seem to be placed as deep in the binding pocket. For wFwLL-NH<sub>2</sub> and wFw-(Isn)-NH<sub>2</sub>, D-Trp<sup>2</sup> may face directly into the receptor pocket, whereas for the hexapeptides, the D-Trp<sup>2</sup> is suggested to face toward TM-II, TM-VI, and TM-VII. Nevertheless, the peptides still show the L-shaped form described in previous studies.<sup>22,23,25</sup>

In modeling studies of the analogues of KwFwLL-NH<sub>2</sub>, Lys<sup>1</sup> and the adjacent aromatic amino acid at position 2 point



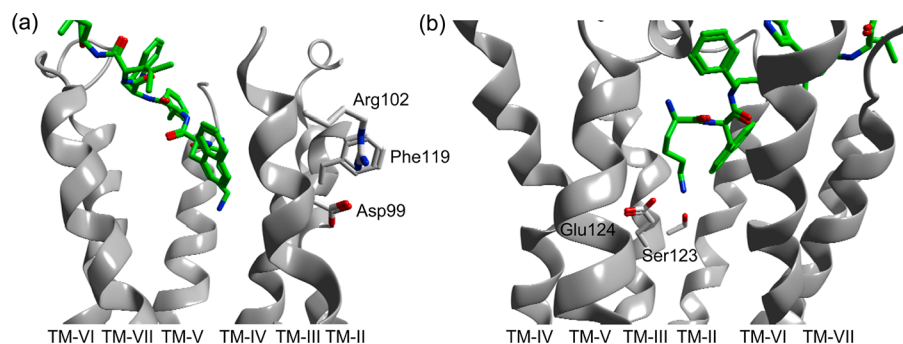


**Figure 9.** Computational modeling of the interaction of (a) Phe119 and (b) Ser123 with K-(D-1-Nal)-FwLL-NH<sub>2</sub> (3). For Phe119, no direct interaction with the peptide could be determined. Moreover, interaction of Phe119 with Asp99 and Arg102 could be possible. In contrast, Ser123 seems to interact directly with Lys<sup>1</sup> of the peptide.

slightly to each other. The two nitrogens of the L-Lys<sup>1</sup> side chain and the D-Trp<sup>2</sup> side chain are prone to repulse each other. This repulsion does not exist for D-Dip<sup>2</sup> (5) and D-1-Nal<sup>2</sup> (3) and can be the reason for their higher inverse agonistic efficacies. We could then assume that the sulfur contained in D-Bth<sup>2</sup> can lead to an electrostatic interaction with Lys<sup>1</sup> and thus explain the very high potency and inverse agonist efficacy of peptide 4. In contrast, both agonists 17 and 18 contain a D-Trp at position 2. Moreover, we could observe an increased attraction between L-Phe<sup>3</sup> and D-2-Nal<sup>4</sup> (17) compared to other amino acids at position 4, which could favor agonistic activity. By the different interactions, the conformations of the hexapeptides can be slightly changed, inducing a changed binding to the receptor and a changed efficacy and/or potency.

For the stabilization of the active or the inactive receptor conformation, Trp276 is proposed to be the crucial residue in the highly conserved CWxP region acting as a rotamer switch in the ghrelin receptor. The lateral indole chain of the Trp is suggested to undergo a rotation from TM-III/TM-IV to TM-III/TM-V, resulting in an inward movement of TM-VI to get in the active conformation.<sup>35,36</sup> Because of this rotation, Trp276 and Phe221 are close to each other and can make aromatic–aromatic interactions that stabilize the active conformation.<sup>37</sup> The hexapeptides in this study did not show a direct interaction with Trp276, implying an indirect influence on the CWxP rotamer switch region. Interestingly, the peptides are undergoing interactions with an aromatic cluster of Phe279, Phe309, and Phe312 in TM-VI and TM-VII. These amino acids are described as very likely to undergo interactions because of their proximity and thereby to stabilize the active conformation.<sup>10</sup> By the addition of a ligand, these contacts can be disturbed, resulting in a destabilization of the active conformation. Our modeling studies suggest that Phe279 and Phe309 can interact with the amino acid at position 2. Moreover, the slightly different sizes of the residues at positions 2 and 4 of the hexapeptide can interact differently with the receptor, stabilizing the active or the inactive conformation of the receptor. The inactive conformation is stabilized by an increased bi- or dicyclic residue at position 2 (D-1-Nal (3), D-Bth (4), and D-Dip(5)) compared to D-Trp. An increased bicyclic residue at position 4 (D-2-Nal (17) and D-1-Nal (18)) compared to D-Trp pushes the receptor to its active conformation.

To evaluate receptor–ligand interaction, we compared modeling and mutagenesis studies (Figure 9). In previous mutagenesis studies, Gln120, Ser123, Phe279, Arg283, and Phe309 were major hits for the inverse agonist KwFwLL-NH<sub>2</sub>

and/or the agonist AwFwLL-NH<sub>2</sub><sup>23</sup> and are predicted to be in proximity to the ligand. Ser123 seems to interact with the NH<sub>3</sub><sup>+</sup> of the Lys<sup>1</sup> side chain, and we therefore tested K-(D-1-Nal)-FwLL-NH<sub>2</sub> (3) with different Ser123 mutants. With Asp, Tyr, and Thr at position 123, electrostatic interactions were maintained and the peptide acted as an inverse agonist with a potency comparable to that of the wild type or only slightly decreased. In contrast, with the mutant Ser123:Ala no response could be observed. Interestingly, with KwFwLL-NH<sub>2</sub> no change in potency could be found in previous studies between the wild-type receptor and the Ser123:Ala mutant,<sup>23</sup> emphasizing the hypothesis that D-1-Nal at position 2 induces a different conformation of the Lys<sup>1</sup>. For the agonist KwF-(D-2-Nal)-LL-NH<sub>2</sub> (17), we could not observe a switch in potency or efficacy, although the agonist AwFwLL-NH<sub>2</sub> was turned into an inverse agonist by this mutation.<sup>23</sup> This could be the result of a different agonist/inverse agonist inducing action of the Lys and the Ala side chain. The combined data of mutagenesis and modeling suggest that the Lys side chain of the hexapeptide indeed interacts with Ser123 directly and may be one important player for the switch between agonism and inverse agonism. Moreover, the mutagenesis data of peptide 17 are consistent with the previous data of the lead peptide because of their shared N-terminal part. For both peptides, no change of efficacy could be observed. Interestingly, KwFwLL-NH<sub>2</sub> acts as an inverse agonist and KwF-(D-2-Nal)-LL-NH<sub>2</sub> acts as an agonist, implying an efficacy switch region in the ghrelin receptor binding the wFw core of the peptide.

Some residues also appeared to have indirect influences on the peptide behavior. In this study, Asp99 and Phe119 are predicted to face toward each other and not to directly interact with the ligand. Moreover, Phe119 seems to interact with Arg102 by cation– $\pi$  interactions. Nevertheless, mutation of Phe119 had different influences on the hexapeptides. With a Phe119:Ser mutant, the response of K-(D-1-Nal)-FwLL-NH<sub>2</sub> was swapped from inverse agonism to agonism and a decrease of potency could be observed (3.8 nM vs 237.6 nM). Interestingly, the behavior of KwF-(D-2-Nal)-LL-NH<sub>2</sub> is not altered. Similar results were obtained in previous studies. Peptide characteristics of KwFwLL-NH<sub>2</sub> were switched from inverse agonism to agonism with the Phe119:Ser mutant, although peptide potency was only slightly decreased. In contrast, this mutant did not influence the behavior of AwFwLL-NH<sub>2</sub>.<sup>23</sup> Because of the changes induced by the mutation, we propose that electrostatic interactions between Ser119 and Arg102 may change the receptor conformation and thus modify the peptide response, although no direct



interaction occurred between Phe119 and the ligand. Thereby, Phe119 may play an important indirect role for activation of the receptor.

In conclusion, we created potent agonists and inverse agonists at the ghrelin receptor and revealed a tripeptide switch region of KwFwLL-NH<sub>2</sub> able to induce agonism and inverse agonism. The most potent inverse agonist K-(D-1-Nal)-FwLL-NH<sub>2</sub> and the most potent agonist KwF-(D-2-Nal)-LL-NH<sub>2</sub> emphasize the sensitivity of the switch region. Indeed, only minor changes in the aromatic core wFw could modulate the peptide behavior. In addition, inverse agonism and agonism appeared to be additive effects and are possibly induced by different binding affinities. Furthermore, mutagenesis studies could prove that Phe119 and Ser123 at the receptor are key positions for the agonist and inverse agonist response of the hexapeptides. Acute food intake studies with the inverse agonist K-(D-1-Nal)-FwLL-NH<sub>2</sub> demonstrated its influence on food intake and thereby supports the hypothesis that those hexapeptides are indeed promising compounds for obesity treatment.

## MATERIALS AND METHODS

**Materials.** Ghrelin was obtained from PolyPeptides (Hillerød, Denmark). N<sup>α</sup>-Fmoc-protected amino acids were purchased from Bachem (Bubendorf, Switzerland) and Iris Biotech GmbH (Marktredwitz, Germany). The side chain protecting group for Lys and Trp was *tert*-butyloxycarbonyl (Boc). 4-(2',4'-Dimethoxyphenyl)-9-fluorenylmethoxycarbonylaminoethyl)phenoxy (Rink amide) resin and 1-hydroxybenzotriazole (HOBt) were purchased from Novabiochem (Schwalbach, Germany). N',N'-Diisopropylcarbodiimide (DIC) and acetonitrile (for HPLC) were purchased from Sigma-Aldrich (Taufkirchen, Germany). Trifluoroacetic acid (TFA), *tert*-butanol, methanol, thioanisole, and 1,2-ethanedithiol were obtained from Fluka (Taufkirchen, Germany). Diethyl ether, dichloromethane, methanol, and dimethylformamide (DMF) were purchased from Biosolve (Valkenswaard, The Netherlands).

For cell culture, inositol trisphosphate turnover assay, and competitive binding assay, the following media and supplements were used: DMEM with higher glucose (4.5 g/L) with L-glutamine, phosphate buffered saline (PBS), bovine serum albumin (BSA), and penicillin and streptomycin, which were purchased from PAA Laboratories (Pasching, Austria). Hygromycin B was obtained from InvivoGen Europe (Toulouse, France). Trypsin-EDTA and fetal calf serum (FCS) were obtained from Gibco Life Technologies (Basel, Switzerland). Metafectene was purchased from Biontech Laboratories GmbH (Martinsried, Germany). [2-<sup>3</sup>H(N)]Myo-inositol, <sup>125</sup>I-His-ghrelin, and scintillation cocktail Optiphase Hisafe 3 were obtained from PerkinElmer (Rodgau, Germany). Sodium hydroxide (NaOH) and formic acid (HCOOH) were purchased from Grüssing GmbH (Filsum, Germany). Sodium formate and disodium tetraborate decahydrate were obtained from MERCK (Darmstadt, Germany). EDTA disodium salt dehydrate was purchased from AppliChem (Darmstadt, Germany). Anti-FLAG antibody (catalog no. F1804) and lithium chloride (LiCl) were from Sigma (Taufkirchen, Germany). Ammonium formate was obtained from Paul Lohmann GmbH (Emmerthal, Germany). Pefabloc SC was from Fluka (Taufkirchen, Germany). Anti-mouse IgG horseradish peroxidase (HRP) linked antibody (catalog no. 32430) was obtained from Thermo Scientific (Waltham, MA, U.S.) and tetramethylbenzidine from Kem-En-Tec (Taastrup, Denmark).

**Peptide Synthesis.** The synthesis of the hexapeptides was performed on solid support with an automated multiple peptide synthesizer (Syrto, MultiSynTech, Bochum, Germany) by using Rink amide resin (13.5 μmol) and Fmoc/*t*-Bu strategy as described recently.<sup>24</sup> Special amino acids were coupled manually with 5 equiv of Fmoc amino acid, 5 equiv of DIC, and 5 equiv of HOBt in DMF. The elongated peptides were cleaved from the resin in one step with

90% TFA and scavenger (thioanisole/1,2-ethanedithiol, 7:3 (v/v)) and precipitated with an ice-cold mixture of hexane/diethyl ether (3:1 (v/v)). After the washing steps, the peptides were finally lyophilized. Purification of the peptides was achieved with preparative HPLC on a reversed-phase C18 column (Phenomenex Jupiter 10u Proteo 90 Å: 250 mm × 21.2 mm, 7.8 μm, 90 Å) with a flow rate of 10 mL/min and λ = 220 nm. A linear gradient of solvent B in solvent A (solvent A = water + 0.1% TFA; solvent B = acetonitrile + 0.08% TFA) was used depending on the peptides. Peptides were analyzed by MALDI-MS (UltraflexII, Bruker, Bremen, Germany). Purity of the peptides was determined by analytical reversed-phase HPLC on columns VariTide RPC (Varian, 250 mm × 4.6 mm, 6 μm, 200 Å) and Phenomenex Jupiter 4u Proteo 90 Å (Phenomenex, 250 mm × 4.6 mm, 4 μm, 90 Å). A linear gradient of 20–70% B in A in 40 min (solvent A = water + 0.1% TFA; solvent B = acetonitrile + 0.08% TFA) with a flow rate of 0.8 and 0.6 mL/min was used (λ = 220 nm), respectively. The observed masses were in full agreement with the calculated masses, and peptides with a purity of ≥95% could be obtained according to the analytical HPLC.

**Molecular Biology.** The human ghrelin receptor DNA was obtained in pcDNA3.1 vector (Mike Brownstein, NIH, Maryland). Receptor DNA was cloned into pEYFP-N1 (Clontech Europe, Heidelberg, Germany) in order to fuse EYFP C-terminally to the receptor with appropriate restriction endonucleases (Sall and BamHI). The ghrelin receptor EYFP fusion gene was subcloned into the eukaryotic expression plasmid pVito2-hygro-mcs (InvivoGen Europe, Toulouse, France) via Sall and AvrII. The sequence was verified by sequencing. Mutations were introduced using overlap extension PCR as described previously.<sup>23,38</sup> The PCR products were digested with appropriate restriction endonucleases (BamHI and EcoRI), purified, and cloned into the vector pCMV-Tag2B. All reactions were carried out using *Pfu* polymerase (Stratagene, La Jolla, CA) according to the instructions of the manufacturer. All mutations were verified by DNA sequence analysis.

**Cell Culture and Transfection.** Peptides were tested in COS7 cells, either transiently or stably transfected with the ghrelin receptor. EC<sub>50</sub> values and efficacy of peptides tested with the stable or transiently transfected cells were comparable. COS7 cells were grown in a humidified atmosphere at 37 °C and 5% CO<sub>2</sub> in Dulbecco's modified Eagle's medium with higher glucose supplemented with 10% (v/v) FCS and 1% (v/v) penicillin/streptomycin. COS7 cells were seeded in 24-well plates (80000–100000 cells/well) in DMEM with 10% FCS. For stable cells, the medium contained 0.4 mg/mL hygromycin B. For transient transfection, COS7 cells were incubated for 14 h with the ghrelin receptor DNA. Each well was treated with 0.3 μg of DNA and 0.9 μL of metafectene.

**Inositol Trisphosphate Turnover Assay.** The day after transfection or the day after seeding for stable cells, cells were incubated with [2-<sup>3</sup>H]myo-inositol (2 μCi/mL). Stimulation was then carried out with seven to nine different peptide concentrations and stopped by aspirating the medium. After cell lysis, cell debris was removed and the supernatant was purified on an anion-exchange resin (Bio-Rad AG 1-X8).<sup>23,24</sup> The obtained data were analyzed with GraphPad Prism 3.0 (GraphPad Software, San Diego, CA, U.S.). Therefore, dpm values are assigned to the corresponding peptide concentrations. Nonlinear regression was used to obtain sigmoidal curves. For better comparability, dpm values were normalized to the constitutive activity. Constitutive activity of 100% represents the basal activity, the activity of the receptor without the influence of peptides. E<sub>max</sub> is the efficacy of the peptide and represents the difference between constitutive activity and activity at maximal effect of the peptide. EC<sub>50</sub> is the peptide concentration at half-maximal effect.

**Receptor Binding Studies.** For competitive binding assays, with ghrelin receptor stably transfected COS7 cells were resuspended in incubation buffer (DMEM containing 50 mM Pefabloc SC and 1% BSA). Peptide solutions (10<sup>-5</sup>–10<sup>-10</sup> M or 10<sup>-6</sup>–10<sup>-11</sup> M) were prepared in water containing 1% BSA and incubated with 200 μL of cell suspension containing about 10 000 cells. For the assay conditions, a K<sub>D</sub> of 144.8 pM was determined for <sup>125</sup>I-His-ghrelin. Incubation was performed for 75 min at room temperature and terminated by

centrifugation at 4 °C for 5 min. Cell pellets were washed twice with ice cold phosphate buffered saline (PBS), centrifuged, and resuspended in 100  $\mu$ L of ice cold PBS. The cell suspension was mixed with scintillation cocktail, and radioactivity was measured in a scintillation counter. Each experiment was performed in triplicate. IC<sub>50</sub> values of the binding curves were calculated by nonlinear regression on a sigmoidal dose-response based model by using the program GraphPad Prism 3.0.  $K_i$  values were calculated by Cheng–Prusoff equation. Values in column diagram were normalized over basal dpm and dpm with 10<sup>-6</sup> M ghrelin.

**Expression Analysis.** An ELISA assay was used to evaluate cell surface expression of receptor variants. Therefore, COS7 cells were transiently transfected with N-terminally FLAG-tagged receptor constructs. On the next day, cells were seeded in 96-well plate with 3.5  $\times$  10<sup>5</sup> cells per well. After incubation overnight, cells were fixed with 3.7% formaldehyde in PBS and washed thoroughly with PBS. Unspecific binding sites were blocked with 3% nonfat dry milk in PBS (blocking buffer). Anti-FLAG antibody was diluted 1:1000 in blocking buffer (primary antibody) and anti-mouse IgG horseradish peroxidase (HRP) linked antibody diluted 1:1250 in 1.5% nonfat dry milk in PBS (secondary antibody). HRP activity was assessed using tetramethylbenzidine. The reaction was terminated with 0.5 M sulfuric acid. The color reaction product was transferred into a clear 96-well plate and the absorbance at 450 nm measured. The mean absorbance for mock-transfected cells was subtracted as a background cutoff. The expression level was estimated as a ratio between absorbance mean values for the receptor construct and the wild-type receptor measured in the same assay.<sup>39</sup>

**Modeling.** A multiconformational docking setup was employed, where different conformations of the receptor are generated by a set of refined homology models represented by different template structures, packing of side chains, and loop conformations to provide insight into ligand-bound receptor conformations. Initially, four comparative homology models of the human ghrelin receptors were constructed from pairwise sequence alignments to each of the four X-ray structures, bovine rhodopsin (PDB entry 1F88),<sup>40</sup> dopamine D3 (PDB entry 3PBL),<sup>41</sup> the  $\beta$ 1-adrenergic receptor (PDB entry 2VT4),<sup>42</sup> and the adenosine A2A receptor (PDB entry 3EML),<sup>43</sup> using the ICM packages<sup>44</sup> (Molsoft, LLC, La Jolla, CA).

The sequence identity between the ghrelin receptor and the template structures bovine rhodopsin, adenosine A2a,  $\beta$ 1-adrenergic receptor, and the dopamine D3 receptor is 19%, 28%, 24%, and 20%, respectively. Since the quality of comparative homology models is highly dependent on the quality of the pairwise sequence alignment, manual inspections and adjustment were performed to ensure proper alignment of conserved class A GPCR generic fingerprints and to avoid gaps in the transmembrane region (Supporting Information Figure S1). Specifically, the highly conserved Cys116 in the extracellular part of TMIII and Cys198 in extracellular loop 2, which are formed in most 7TM receptors, were manually aligned to the template structures to ensure that the disulfide bridge would be formed in the initial ghrelin homology model. During ghrelin model generation, all amino acids were subjected to a full side chain optimization to optimize their packing. Loop regions of the ghrelin model, which were constructed without a template, were initially assigned the best scored loop conformation obtained from similar “fragments” in ICMs database of experimental structures.

The ghrelin receptor is capable of recognizing a vast number of very different small molecule agonists and antagonists (with respect to size, chemical scaffolds, and distribution of chemical features) besides a large number of very different peptides and truncated or modified variants of the endogenous ligand. To recognize such a variety of compounds, the receptor has to exist in multiple conformational states coupled to ligand type and receptor activity. Moreover, intrinsic flexibility of known GPCR structures addresses the necessity of docking into a receptor ensemble. Thus, the four resulting homology models were subjected to full-atom structure relaxation in Rosetta (version 3.2.1),<sup>45–47</sup> which originally was developed to address the protein folding problem and later extended to focus on the design of

protein structures, protein folding mechanisms, protein–protein interactions, and docking<sup>40,42,48</sup> using the membrane force field.<sup>46,49</sup>

In brief the relax protocol involves (1) generation and optimization of the extracellular loops, using a combination of the cyclic coordinate descent (CCD)<sup>50</sup> and kinematic closure (KIC)<sup>51</sup> application and (2) repacking of backbone and side chains using the relax protocol. During model refinement, a disulfide bridge between Cys116(III:01) and Cys198 in the ELC2 was defined; otherwise loops were modeled ab initio. Fragment files were obtained from the Robetta server (www.robetta.org). A detailed explanation of the CCD and KIC algorithms can be found elsewhere.<sup>50,51</sup> In brief, the goal of both algorithms is to explore the conformational space of structural variable regions (loop) initially using a centroid representation of protein side chains and explicit backbone representation, followed by a higher-resolution search using all atoms. In the initial stage, loops are generated by a fragment buildup/insertion Monte Carlo algorithm where CCD is used to close the loop at the end of the simulation. In each step of the Monte Carlo cycle KIC is used to refine the structures where all residues within the neighbor distance of a loop are repacked and then subjected to side chain rotamer trials. The backbone and side chains of all loop residues and neighboring residues are then followed by a line minimization of the loop  $\varphi/\psi$  torsions, and the final conformations are accepted/rejected by the Metropolis criterion using the full-atom Rosetta scoring function. A total of 1000 ghrelin models were generated from each of the initial homology.

The top 50% of the best scored models were extracted from each of the four simulations. The resulting structures for the individual receptor variants were clustered with respect to the backbone conformation of the extracellular half of the transmembrane helices and extracellular loops (excluding extracellular loop 2a) using Rosetta's cluster routine and a 1.0 Å rmsd cluster threshold. The lowest energy structure from the top 15 most populated clusters was extracted from each simulation, producing a total ensemble of 60 ghrelin receptor models. This ensemble of structures seems to be large compared to the number of conformations applied in recent studies.<sup>52–54</sup> However, the result of a “large” receptor ensemble is an attempt to address conformational properties of the extracellular loops which are believed to be important for the various studies peptides. Importantly, the transmembrane region of the individual structures in the ensemble have a  $C\alpha$  root-mean-square deviation of <3 Å to any of the 14 distinct class A GPCR structures determined to date.

**Docking to Ghrelin Receptor Ensemble.** Finally, fully flexible ligand docking to each of the 60 receptor models was performed by ICM biased probability Monte Carlo docking routine under softened van der Waals (vdW) conditions using 4D grids represented by six grid potentials of 0.5 Å spacing, including three van der Waals grid potentials for a carbon probe, large atom probe, or hydrogen probe, a hydrogen bonding grid potential, an electrostatic grid potential, and a hydrophobic grid potential ICM<sup>55,56</sup> and thoroughness parameter of 3. The docking grids were defined to encompass a binding pocket described by all corresponding receptor residues within 4.5 Å of the ligands in the template crystal structures,<sup>40,42,43,48</sup> when superimposed onto the stack of generated ghrelin receptor models. The final docking grid was extended approximately 8 Å toward TM-I and TM-II to allow the longer ligands to occupy and interact with pocket located between TM-II, TM-III, and TM-VII. Individual best scored docking poses were subsequently optimized using a combined Monte Carlo and minimization procedure (using the MMFF94 force field), keeping ligand and surrounding protein residues (in an 8 Å radius from the starting position) flexible. All backbone coordinates were held fixed. Two rounds of optimization were performed: an initial refinement under a softened van der Waals potential and a second refinement with the full van der Waals potential. A final stack of 50 conformations was generated that were scored and manually analyzed to identify the complexes between the peptide ligands and the ghrelin receptor.

**Docking Pose Elucidation.** In general, comparative homology models are considered to be associated with atomic position errors, which impede their use for purposes that require atomic-resolution data, such as drug design and protein–ligand interaction predictions. Furthermore, minor inaccuracies in the structural models due to lack

of explicit water molecules, approximations in the Rosetta force field, and proper conformational sampling in combination with an expected relatively small energy gap between the “correct” and “incorrect” docking poses may challenge the use of ligand–protein interaction energies for accurate determination of docking poses. From this realization, the ensemble of ligand receptor complexes was evaluated based on docking scores and mutational mapping data and the possibility of the studied peptides to interact with residues in the binding pocket between the transmembrane helices, e.g., Glu124, which previously has been identified to be an important anchor point for a variety of small molecule and peptide ligands.<sup>33</sup>

**Acute Feeding Study in Rats.** For *in vivo* studies, peptide 3 was delivered intracerebroventricularly. The rats were stereotaxically implanted with a stainless steel cannula (Holm Finmekanik AS, Copenhagen, Denmark) aimed at the right lateral ventricle 1 mm caudal and 1.5 mm lateral to bregma and 4 mm ventral to cranium externa. Rats were left to recover in the metabolic cages (MANI Feed Win, Ellegaard Systems) for adaptation for at least 5 days, only interrupted by daily handling and body weight measurements. With these cages we could accurately measure the food and water intake of rats for up to 48 h. The powdered diet used eliminated food hoarding and spill. Cannula placement was confirmed by measuring the drinking response to angiotensin injection (100 nmol/rat). Administration of peptide was done with 1 nmol/rat ( $n = 6$ ). As a negative control, a vehicle solution of 0.9% saline with DMSO ( $n = 7$ ) was used.

## ■ ASSOCIATED CONTENT

### ● Supporting Information

Analytical data with RP-HPLC retention times and molecular mass of the synthesized peptides; pairwise alignment of the ghrelin receptor with bovine rhodopsin receptor, adenosine A2A receptor, dopamine D3 receptor, and  $\beta$ 1-adrenergic receptor for computational modeling. This material is available free of charge via the Internet at <http://pubs.acs.org>.

## ■ AUTHOR INFORMATION

### Corresponding Author

\*Phone: 0049-341-9736900. E-mail: [beck-sickinger@uni-leipzig.de](mailto:beck-sickinger@uni-leipzig.de).

### Notes

The authors declare no competing financial interest.

## ■ ACKNOWLEDGMENTS

The authors express their thanks to Regina Reppich-Sacher and Kristin Löbner. We gratefully acknowledge the Graduate School “Leipzig School of Natural Sciences, Building with Molecules and Nano-Objects” (BuildMoNa), the Humboldt Foundation, the IFB-K-18, and GIPIO (Grant No. 223057) for generous funding. The Novo Nordisk Foundation Center for Basic Metabolic Research ([www.metabol.ku.dk](http://www.metabol.ku.dk)) is supported by an unconditional grant from the Novo Nordisk Foundation to the University of Copenhagen.

## ■ ABBREVIATIONS USED

AgRP, agouti-related peptide; Boc, *tert*-butyloxycarbonyl; DIC, *N,N'*-diisopropylcarbodiimide; DMF, dimethylformamide; ECL, extracellular loop; EYFP, enhanced yellow fluorescent protein; FCS, fetal calf serum; Fmoc, *N*-(9-fluorenyl)-methoxycarbonyl; GHS-R, growth hormone secretagogue receptor; GPCR, G-protein-coupled receptor; HOBt, 1-hydroxybenzotriazole; MSP, modified substance P; NPY, neuropeptide Y; SAR, structure–activity relationship; TFA, trifluoroacetic acid; TM, transmembrane

## ■ REFERENCES

- (1) Howard, A. D.; Feighner, S. D.; Cully, D. F.; Arena, J. P.; Liberato, P. A.; Rosenblum, C. I.; Hamelin, M.; Hreniuk, D. L.; Palyha, O. C.; Anderson, J.; Paress, P. S.; Diaz, C.; Chou, M.; Liu, K. K.; McKee, K. K.; Pong, S. S.; Chaung, L. Y.; Elbrecht, A.; Dashkevich, M.; Heavens, R.; Rigby, M.; Sirinathsinghji, D. J.; Dean, D. C.; Melillo, D. G.; Patchett, A. A.; Nargund, R.; Griffin, P. R.; DeMartino, J. A.; Gupta, S. K.; Schaeffer, J. M.; Smith, R. G.; Van der Ploeg, L. H. A receptor in pituitary and hypothalamus that functions in growth hormone release. *Science* **1996**, *273*, 974–977.
- (2) Kojima, M.; Hosoda, H.; Date, Y.; Nakazato, M.; Matsuo, H.; Kangawa, K. Ghrelin is a growth-hormone-releasing acylated peptide from stomach. *Nature* **1999**, *402*, 656–660.
- (3) Tschöp, M.; Smiley, D. L.; Heiman, M. L. Ghrelin induces adiposity in rodents. *Nature* **2000**, *407*, 908–913.
- (4) Nakazato, M.; Murakami, N.; Date, Y.; Kojima, M.; Matsuo, H.; Kangawa, K.; Matsukura, S. A role for ghrelin in the central regulation of feeding. *Nature* **2001**, *409*, 194–198.
- (5) Gnanapavan, S.; Kola, B.; Bustin, S. A.; Morris, D. G.; McGee, P.; Fairclough, P.; Bhattacharya, S.; Carpenter, R.; Grossman, A. B.; Korbonits, M. The tissue distribution of the mRNA of ghrelin and subtypes of its receptor, GHS-R, in humans. *J. Clin. Endocrinol. Metab.* **2002**, *87*, 2988.
- (6) Guan, X. M.; Yu, H.; Palyha, O. C.; McKee, K. K.; Feighner, S. D.; Sirinathsinghji, D. J.; Smith, R. G.; Van der Ploeg, L. H.; Howard, A. D. Distribution of mRNA encoding the growth hormone secretagogue receptor in brain and peripheral tissues. *Brain Res.* **1997**, *48*, 23–29.
- (7) Lopez, M.; Lage, R.; Saha, A. K.; Perez-Tilve, D.; Vazquez, M. J.; Varela, L.; Sangiao-Alvarellos, S.; Tovar, S.; Raghay, K.; Rodriguez-Cuenca, S.; Deoliveira, R. M.; Castaneda, T.; Datta, R.; Dong, J. Z.; Culler, M.; Sleeman, M. W.; Alvarez, C. V.; Gallego, R.; Lelliott, C. J.; Carling, D.; Tschöp, M. H.; Dieguez, C.; Vidal-Puig, A. Hypothalamic fatty acid metabolism mediates the orexigenic action of ghrelin. *Cell Metab.* **2008**, *7*, 389–399.
- (8) Tups, A.; Helwig, M.; Khoroshii, R. M.; Archer, Z. A.; Klingenspor, M.; Mercer, J. G. Circulating ghrelin levels and central ghrelin receptor expression are elevated in response to food deprivation in a seasonal mammal (*Phodopus sungorus*). *J. Neuroendocrinol.* **2004**, *16*, 922–928.
- (9) Wren, A. M.; Seal, L. J.; Cohen, M. A.; Brynes, A. E.; Frost, G. S.; Murphy, K. G.; Dhillo, W. S.; Ghatei, M. A.; Bloom, S. R. Ghrelin enhances appetite and increases food intake in humans. *J. Clin. Endocrinol. Metab.* **2001**, *86*, 5992.
- (10) Holst, B.; Holliday, N. D.; Bach, A.; Elling, C. E.; Cox, H. M.; Schwartz, T. W. Common structural basis for constitutive activity of the ghrelin receptor family. *J. Biol. Chem.* **2004**, *279*, 53806–53817.
- (11) Petersen, P. S.; Woldbye, D. P.; Madsen, A. N.; Egerod, K. L.; Jin, C.; Lang, M.; Rasmussen, M.; Beck-Sickinger, A. G.; Holst, B. *In vivo* characterization of high basal signaling from the ghrelin receptor. *Endocrinology* **2009**, *150*, 4920–4930.
- (12) Damian, M.; Marie, J.; Leyris, J. P.; Fehrentz, J. A.; Verdier, P.; Martinez, J.; Baneres, J. L.; Mary, S. High constitutive activity is an intrinsic feature of ghrelin receptor protein: a study with a functional monomeric GHS-R1a receptor reconstituted in lipid discs. *J. Biol. Chem.* **2012**, *287*, 3630–3641.
- (13) Holst, B.; Schwartz, T. W. Constitutive ghrelin receptor activity as a signaling set-point in appetite regulation. *Trends Pharmacol. Sci.* **2004**, *25*, 113–117.
- (14) Rokholm, B.; Baker, J. L.; Sorensen, T. I. The levelling off of the obesity epidemic since the year 1999—a review of evidence and perspectives. *Obes. Rev.* **2010**, *11*, 835–846.
- (15) Hofbauer, K. G.; Nicholson, J. R. Pharmacotherapy of obesity. *Exp. Clin. Endocrinol. Diabetes* **2006**, *114*, 475–484.
- (16) Cooke, D.; Bloom, S. The obesity pipeline: current strategies in the development of anti-obesity drugs. *Nat. Rev. Drug Discovery* **2006**, *5*, 919–931.



- (17) Chollet, C.; Meyer, K.; Beck-Sickingler, A. G. Ghrelin—a novel generation of anti-obesity drug: design, pharmacomodulation and biological activity of ghrelin analogues. *J. Pept. Sci.* **2009**, *15*, 711–730.
- (18) Hatef, D. A.; Trussler, A. P.; Kenkel, J. M. Procedural risk for venous thromboembolism in abdominal contouring surgery: a systematic review of the literature. *Plast. Reconstr. Surg.* **2010**, *125*, 352–362.
- (19) Colucci, R. A. Bariatric surgery in patients with type 2 diabetes: a viable option. *Postgrad. Med.* **2011**, *123*, 24–33.
- (20) Berthoud, H. R.; Shin, A. C.; Zheng, H. Obesity surgery and gut–brain communication. *Physiol. Behav.* **2011**, *105*, 106–119.
- (21) Holst, B.; Cygankiewicz, A.; Jensen, T. H.; Ankersen, M.; Schwartz, T. W. High constitutive signaling of the ghrelin receptor—identification of a potent inverse agonist. *Mol. Endocrinol.* **2003**, *17*, 2201–2210.
- (22) Holst, B.; Lang, M.; Brandt, E.; Bach, A.; Howard, A.; Frimurer, T. M.; Beck-Sickingler, A.; Schwartz, T. W. Ghrelin receptor inverse agonists: identification of an active peptide core and its interaction epitopes on the receptor. *Mol. Pharmacol.* **2006**, *70*, 936–946.
- (23) Holst, B.; Mokrosinski, J.; Lang, M.; Brandt, E.; Nygaard, R.; Frimurer, T. M.; Beck-Sickingler, A. G.; Schwartz, T. W. Identification of an efficacy switch region in the ghrelin receptor responsible for interchange between agonism and inverse agonism. *J. Biol. Chem.* **2007**, *282*, 15799–15811.
- (24) Els, S.; Beck-Sickingler, A. G.; Chollet, C. Ghrelin receptor: high constitutive activity and methods for developing inverse agonists. *Methods Enzymol.* **2010**, *485*, 103–121.
- (25) Sivertsen, B.; Lang, M.; Frimurer, T. M.; Holliday, N. D.; Bach, A.; Els, S.; Engelstoft, M. S.; Petersen, P. S.; Madsen, A. N.; Schwartz, T. W.; Beck-Sickingler, A. G.; Holst, B. Unique interaction pattern for a functionally biased ghrelin receptor agonist. *J. Biol. Chem.* **2011**, *286*, 20845–20860.
- (26) Holst, B.; Frimurer, T. M.; Mokrosinski, J.; Halkjaer, T.; Cullberg, K. B.; Underwood, C. R.; Schwartz, T. W. Overlapping binding site for the endogenous agonist, small-molecule agonists, and ago-allosteric modulators on the ghrelin receptor. *Mol. Pharmacol.* **2009**, *75*, 44–59.
- (27) Cowley, M. A.; Smith, R. G.; Diano, S.; Tschop, M.; Pronchuk, N.; Grove, K. L.; Strasburger, C. J.; Bidlingmaier, M.; Esterman, M.; Heiman, M. L.; Garcia-Segura, L. M.; Nillni, E. A.; Mendez, P.; Low, M. J.; Sotonyi, P.; Friedman, J. M.; Liu, H.; Pinto, S.; Colmers, W. F.; Cone, R. D.; Horvath, T. L. The distribution and mechanism of action of ghrelin in the CNS demonstrates a novel hypothalamic circuit regulating energy homeostasis. *Neuron* **2003**, *37*, 649–661.
- (28) DeBoer, M. D.; Zhu, X. X.; Levasseur, P.; Meguid, M. M.; Suzuki, S.; Inui, A.; Taylor, J. E.; Halem, H. A.; Dong, J. Z.; Datta, R.; Culler, M. D.; Marks, D. L. Ghrelin treatment causes increased food intake and retention of lean body mass in a rat model of cancer cachexia. *Endocrinology* **2007**, *148*, 3004–3012.
- (29) Strassburg, S.; Anker, S. D.; Castaneda, T. R.; Burget, L.; Perez-Tilve, D.; Pfluger, P. T.; Nogueiras, R.; Halem, H.; Dong, J. Z.; Culler, M. D.; Datta, R.; Tschop, M. H. Long-term effects of ghrelin and ghrelin receptor agonists on energy balance in rats. *Am. J. Physiol.: Endocrinol. Metab.* **2008**, *295*, E78–E84.
- (30) Carpino, P. A.; Ho, G. Modulators of the ghrelin system as potential treatments for obesity and diabetes. *Expert Opin. Ther. Pat.* **2008**, *18*, 1253–1263.
- (31) Hiura, Y.; Takiguchi, S.; Yamamoto, K.; Takahashi, T.; Kurokawa, Y.; Yamasaki, M.; Nakajima, K.; Miyata, H.; Fujiwara, Y.; Mori, M.; Kangawa, K.; Doki, Y. Effects of ghrelin administration during chemotherapy with advanced esophageal cancer patients: a prospective, randomized, placebo-controlled phase 2 study. *Cancer* [Online early access]. DOI: 10.1002/cncr.27430. Published Online: January 26, **2012**.
- (32) Diano, S.; Farr, S. A.; Benoit, S. C.; McNay, E. C.; da Silva, I.; Horvath, B.; Gaskin, F. S.; Nonaka, N.; Jaeger, L. B.; Banks, W. A.; Morley, J. E.; Pinto, S.; Sherwin, R. S.; Xu, L.; Yamada, K. A.; Sleeman, M. W.; Tschop, M. H.; Horvath, T. L. Ghrelin controls hippocampal spine synapse density and memory performance. *Nat. Neurosci.* **2006**, *9*, 381–388.
- (33) Chuang, J. C.; Perello, M.; Sakata, I.; Osborne-Lawrence, S.; Savitt, J. M.; Lutter, M.; Zigman, J. M. Ghrelin mediates stress-induced food-reward behavior in mice. *J. Clin. Invest.* **2011**, *121*, 2684–2692.
- (34) Leggio, L. Role of the ghrelin system in alcoholism: acting on the growth hormone secretagogue receptor to treat alcohol-related diseases. *Drug News Perspect.* **2010**, *23*, 157–166.
- (35) Goze, C.; Berge, G.; M'Kadmi, C.; Floquet, N.; Gagne, D.; Galleyrand, J. C.; Fehrentz, J. A.; Martinez, J. Involvement of tryptophan W276 and of two surrounding amino acid residues in the high constitutive activity of the ghrelin receptor GHS-R1a. *Eur. J. Pharmacol.* **2010**, *643*, 153–161.
- (36) Schwartz, T. W.; Frimurer, T. M.; Holst, B.; Rosenkilde, M. M.; Elling, C. E. Molecular mechanism of 7TM receptor activation—a global toggle switch model. *Annu. Rev. Pharmacol. Toxicol.* **2006**, *46*, 481–519.
- (37) Holst, B.; Nygaard, R.; Valentin-Hansen, L.; Bach, A.; Engelstoft, M. S.; Petersen, P. S.; Frimurer, T. M.; Schwartz, T. W. A conserved aromatic lock for the tryptophan rotameric switch in TM-VI of seven-transmembrane receptors. *J. Biol. Chem.* **2010**, *285*, 3973–3985.
- (38) Ho, S. N.; Hunt, H. D.; Horton, R. M.; Pullen, J. K.; Pease, L. R. Site-directed mutagenesis by overlap extension using the polymerase chain reaction. *Gene* **1989**, *77*, 51–59.
- (39) Mokrosinski, J.; Frimurer, T. M.; Sivertsen, B.; Schwartz, T. W.; Holst, B. Modulation of constitutive activity and signaling bias of the ghrelin receptor by conformational constraint in the second extracellular loop. *J. Biol. Chem.* [Online early access]. Published Online: July 30, **2012**.
- (40) Palczewski, K.; Kumasaka, T.; Hori, T.; Behnke, C. A.; Motoshima, H.; Fox, B. A.; Le, T. I.; Teller, D. C.; Okada, T.; Stenkamp, R. E.; Yamamoto, M.; Miyano, M. Crystal structure of rhodopsin: a G protein-coupled receptor. *Science* **2000**, *289*, 739–745.
- (41) Chien, E. Y.; Liu, W.; Zhao, Q.; Katritch, V.; Han, G. W.; Hanson, M. A.; Shi, L.; Newman, A. H.; Javitch, J. A.; Cherezov, V.; Stevens, R. C. Structure of the human dopamine D3 receptor in complex with a D2/D3 selective antagonist. *Science* **2010**, *330*, 1091–1095.
- (42) Warne, T.; Serrano-Vega, M. J.; Baker, J. G.; Moukhametzianov, R.; Edwards, P. C.; Henderson, R.; Leslie, A. G.; Tate, C. G.; Schertler, G. F. Structure of a beta1-adrenergic G-protein-coupled receptor. *Nature* **2008**, *454*, 486–491.
- (43) Jaakola, V. P.; Griffith, M. T.; Hanson, M. A.; Cherezov, V.; Chien, E. Y.; Lane, J. R.; Ijzerman, A. P.; Stevens, R. C. The 2.6 angstrom crystal structure of a human A2A adenosine receptor bound to an antagonist. *Science* **2008**, *322*, 1211–1217.
- (44) ICM-Pro, version 3.7-2; Molsoft, LLC: San Diego, CA; <http://www.molsoft.com>.
- (45) Barth, P.; Wallner, B.; Baker, D. Prediction of membrane protein structures with complex topologies using limited constraints. *Proc. Natl. Acad. Sci. U.S.A.* **2009**, *106*, 1409–1414.
- (46) Barth, P.; Schonbrun, J.; Baker, D. Toward high-resolution prediction and design of transmembrane helical protein structures. *Proc. Natl. Acad. Sci. U.S.A.* **2007**, *104*, 15682–15687.
- (47) Yarov-Yarovoy, V.; Schonbrun, J.; Baker, D. Multipass membrane protein structure prediction using Rosetta. *Proteins* **2006**, *62*, 1010–1025.
- (48) Cherezov, V.; Rosenbaum, D. M.; Hanson, M. A.; Rasmussen, S. G.; Thian, F. S.; Kobilka, T. S.; Choi, H. J.; Kuhn, P.; Weis, W. I.; Kobilka, B. K.; Stevens, R. C. High-resolution crystal structure of an engineered human beta2-adrenergic G protein-coupled receptor. *Science* **2007**, *318*, 1258–1265.
- (49) Leaver-Fay, A.; Tyka, M.; Lewis, S. M.; Lange, O. F.; Thompson, J.; Jacak, R.; Kaufman, K.; Renfrew, P. D.; Smith, C. A.; Sheffler, W.; Davis, I. W.; Cooper, S.; Treuille, A.; Mandell, D. J.; Richter, F.; Ban, Y. E.; Fleishman, S. J.; Corn, J. E.; Kim, D. E.; Lyskov, S.; Berrondo, M.; Mentzer, S.; Popovic, Z.; Havranek, J. J.; Karanicolas, J.; Das, R.; Meiler, J.; Kortemme, T.; Gray, J. J.; Kuhlman, B.; Baker,

D.; Bradley, P. ROSETTA3: an object-oriented software suite for the simulation and design of macromolecules. *Methods Enzymol.* **2011**, *487*, 545–574.

(50) Chu, K. M.; Chow, K. B.; Leung, P. K.; Lau, P. N.; Chan, C. B.; Cheng, C. H.; Wise, H. Over-expression of the truncated ghrelin receptor polypeptide attenuates the constitutive activation of phosphatidylinositol-specific phospholipase C by ghrelin receptors but has no effect on ghrelin-stimulated extracellular signal-regulated kinase 1/2 activity. *Int. J. Biochem. Cell Biol.* **2007**, *39*, 752–764.

(51) Zhang, L.; Brass, L. F.; Manning, D. R. The Gq and G12 families of heterotrimeric G proteins report functional selectivity. *Mol. Pharmacol.* **2009**, *75*, 235–241.

(52) Reynolds, K. A.; Katritch, V.; Abagyan, R. Identifying conformational changes of the beta(2) adrenoceptor that enable accurate prediction of ligand/receptor interactions and screening for GPCR modulators. *J. Comput.-Aided Mol. Des.* **2009**, *23*, 273–288.

(53) Katritch, V.; Rueda, M.; Abagyan, R. Ligand-guided receptor optimization. *Methods Mol. Biol.* **2012**, *857*, 189–205.

(54) Schlessinger, A.; Geier, E.; Fan, H.; Irwin, J. J.; Shoichet, B. K.; Giacomini, K. M.; Sali, A. Structure-based discovery of prescription drugs that interact with the norepinephrine transporter, NET. *Proc. Natl. Acad. Sci. U.S.A.* **2011**, *108*, 15810–15815.

(55) Bottegoni, G.; Kufareva, I.; Totrov, M.; Abagyan, R. Four-dimensional docking: a fast and accurate account of discrete receptor flexibility in ligand docking. *J. Med. Chem.* **2009**, *52*, 397–406.

(56) Totrov, M.; Abagyan, R. Flexible ligand docking to multiple receptor conformations: a practical alternative. *Curr. Opin. Struct. Biol.* **2008**, *18*, 178–184.